JOURNAL OF MECHANICS OF CONTINUA AND MATHEMATICAL SCIENCES
www.journalimcms.org

ISSN (Online) : 2454 -7190 Vol.-21, No.-09, September (2026) pp 1-16 ISSN (Print) 0973-8975

ENHANCING LASER CUTTING QUALITY OF GALVANIZED IRON THROUGH MULTI-OBJECTIVE OPTIMIZATION USING TOPSIS

Chan Choon Kit[1], R. Sankar[2], C. Rathinasuriyan[3], J. Bharani Chandar[4], K. Karthik[5], Adduri S S M Sitaramamurty[6], Li Minmin[7]

[1] Faculty of Engineering and Quantity Surveying, INTI International University, Malaysia, Persiaran Perdana BBN, Putra Nilai, 71800 Nilai, Negeri Sembilan, Malaysia.

[2] Department of Mechanical Engineering, SRM University, Sonipat-131029, Haryana, India.

[3,4,5] Department of Mechanical Engineering, Vel Tech Rangarajan Dr. Sagunthala R&D Institute of Science and Technology, Avadi, Chennai-62, Tamil Nadu, India.

[6] Department of Mechanical Engineering, Aditya University, Aditya Nagar, ADB Rd, Surampalem, Andhra Pradesh 533437, India.

[7] Faculty of Education, Shinawatra University, Pathum Thani, Thailand.

[7] School of Accounting, Guizhou Qiannan University of Economics Guizhou Province, China.

Email: [1]choonkit.chan@newinti.edu.my, [2]sankar.r@srmuniversity.ac.in, [3]rathinasuriyanphd@gmail.com, [4]bharanichandarj@veltech.edu.in, [5]karthikk@veltech.edu.in, [6]assms.murthy@adityauniversity.in, [7]kittitat.y@siu.ac.th

Corresponding Author: **R. Sankar**

https://doi.org/10.26782/jmcms.2026.08.00001

(Received: June 22, 2026; Revised: September 03, 2026; Accepted: September 14, 2026)

Abstract

A cutting procedure that uses heat energy to cut materials without coming into direct contact with the workpiece is laser cutting. Galvanized steel is favored because of its remarkable durability, which combines steel's strength and formability with resistance to corrosion. The Taguchi technique and TOPSIS, a multi-criteria decision-making model, are applied in this work to determine the optimal laser cutting parameters for enhancing surface quality. This study investigates how Cutting Speed (CS), Laser Power (LP), and Gas Pressure (GP) affect kerf width, surface roughness, and cutting time. To ascertain the influence of each input parameter on the output responses, an ANOVA is performed. The best set of parameters, according to the data, is a gas pressure of 8 bar, a power of 1000 W, and a cutting speed of 18 m/min. After laser cutting under optimal conditions, SEM was employed to view the material's surface topography. Furthermore, the results reveal that the grooves and *surface marks are less apparent, which is indicative of a rather stable melting and material removal process when the conditions are optimal.*

Keywords: Laser cutting, Process Innovation, Galvanised Iron, TOPSIS method, Scanning Electron Microscopy

I. Introduction

Sheet metals, including steel, titanium, and aluminum alloys, are essential constituents due to their relevance in daily merchandise and high-performance uses in maritime, aerospace, automotive, military, construction, and marine sectors [I]. Galvanized steel sheets, a crucial material for lightweight production, are widely employed due to their economic efficiency and superior resistance to rust in the atmosphere relative to iron [II, III]. The sheets of galvanized steel are important structural material, which are widely used in the building industry. It has advantages such as safety to the environment, lightweight, resistance to corrosion, and high strength among others [IV]. On the other hand, galvanized steel sheets are very strong as compared to their weight. This makes them a good way of strengthening deep timbers with apertures and at no extra weight. The zinc coating prevents steel corrosion and ensures an increase in the life period of the beam and reduces the maintenance demands, as well as has the benefit of being able to provide fire resistance [V, VI].

Laser cutting has today become one of the most efficient non-conventional sheet metal cutting methods, which necessitates one to have an understanding of the manner in which the parameters of laser cutting influence the quality of the cut [VII]. It refers to a thermally sensitive process that is used to trim cut different materials. It offers better cut quality and cost management in large batch production [VIII]. It denotes the lateral motion of a laser beam over the cutting material in order to cut the material [IX]. A laser beam consists of special light created through photons generated by gas or solid sources, which are synchronized to a very narrow diameter, making a substantial amount of energy be utilized in cutting or welding. In cases where the power of the beam is not enough to produce a keyhole [X, XI]. The basic concept of laser cutting is to focus a coherent laser beam of varied wavelengths on the workpiece, which conducts the energy released by the laser, and the material at the focal point heats rapidly. In Figure 1, the visual representation of the process is shown.

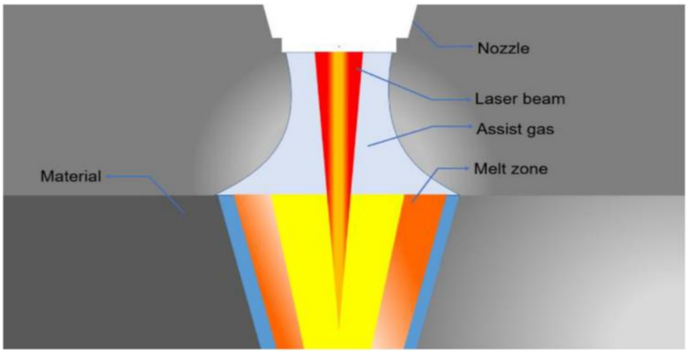

Fig. 1. Laser cutting process [XII]

Hammer et al. [XIII used samples when cutting diverse sheets with different laser shears, one of the fiber lasers and three CO2 lasers. The quantity of particulates generated by the cutting will depend on the type of material, the thickness, and the specifications. It may be the size dispersal, which is reliant on the kind of chemical composition or laser source metal sheets. Parameters of laser cutting have a quantitative and qualitative synergistic effect on the performance of the various processes, such as quality features of the cut, cutting time, removal rate, as well as costs. It is important to determine the best laser cutting parameters that should be used in a particular application.[XIV]

To cut titanium of 4 mm thickness, Alsaadawy et al. [XV used a fiber laser by using the most common parameters identified using Taguchi was accessed via the Minitab program. The impact of cutting velocity, assist GP, and LP on the kerf and surface quality was examined. LP was the primary determinant for surface roughness (SR), followed by cutting velocity and assist GP. Khoshaim et al. [XVI] examined the cutting of PMMA utilizing a continuous CO2 laser beam. The SR is augmented by elevating GP and LP, as well as by reducing thickness and CS. Elevated laser power and reduced CS resulted in the poorest surface SR. Consequently, it is advisable to employ reduced LP and elevated CS to reduce the SR. Kechagia et al. [XVII] examined two standard surface attributes, namely SR and kerf angle, during the laser processing of 3D-printed PLA. Examining the facts revealed that LP is the primary factor influencing the kerf angle, although both LP and velocity significantly affect the SR of the cut. The data dispersion is reduced in the Y direction, indicating that the weaving phenomenon influences laser cutting performance.

The laser cutting process is commonly employed in the automotive production sector. Consequently, identifying and mitigating risks is an ongoing priority of quality and beyond. A set of models and methods developed through study in the field are used to rank these risks [XVIII. Hasan et al. [XIX] have scrutinized the influence of laser parameters on the kerf width of stainless steel. Furthermore, optimal laser cutting parameters that reduce kerf width were determined. It has been discovered that the relationship between LP value, GP, and CS considerably alters the value of the response. Pandya et al. [XX] utilized a CO2 laser to sever MDF panels of three distinct thicknesses. The optimal cutting combinations were presented in favour of high-quality process output and in favour of low cutting cost. As the LP increases, the SR value lowers; similarly, as the CS increases, the SR value also reduces.

Singh et al. [XXI] conducted modeling and parameter optimization during the pulsed CO2 laser cutting of produced hybrid composite sheets using RSM. The fiber laser can effectively cut hybrid composite sheets, achieving superior surface quality on cut edges with appropriate parameter configurations. The regression effects and the linear and quadratic effects of laser cutting factors are essential for model validation. Trajkovicl et al. [XXII] performed an evaluation of the cutting process using three MCDM techniques, including WASPAS, TOPSIS, and EDAS. The experiments came to the conclusion that with the existing model of laser cutting MCDM, higher CS are preferred, and assist GP does not have a significant influence on the net ranking of options. Under such a situation, the MCDM technique can offer a useful tool which helps in determining the most appropriate solutions. Najjar et al. [XXIII] have enriched their AI model to predict the attributes of the kerf quality in the laser cutting of polymer composites. The experimental design was developed using RSM. The model includes Long Short-Term Memory (LSTM) and the Chimp Optimization Algorithm (CHOA). The accuracy of the models was evaluated and compared with the use of different statistical measures. The predictions carried out with LSTM-CHOA were successful due to the presence of the factors of the quality of kerf cuts in the composites despite their being heterogeneous and anisotropic in their structure [XXIV, XXV, XXVI]

This research paper introduces a multi-objective optimization technique in a systematic manner so that the cutting efficiency of galvanized steel sheets through a laser cutter can be optimized. Unlike many of the previous studies that are focused only on the optimization of a single response, this one is focused on simultaneous multipresent performance responses using a Taguchi-TOPSIS hybrid optimization technique. This holistic approach makes it easy to establish the best machining parameters that satisfy the productivity and quality requirements. The study proposes a novel approach of optimization framework for galvanized iron sheets, which have been comparatively neglected to be investigated in the optimization of parameters of laser cutting, although they have vast applications in the construction and manufacturing industries.

II. Experimental Study

The experiments are performed with the help of a D-Fast 1530 -1.5 kW Fiber Laser Cutting Machine that has a nominal output power of 1500 W in constant. The material used as a workpiece is galvanized iron sheets of 3 mm thickness. IPG Photonics laser sources are used in the D-Fast series. The gas used is nitrogen-assist gas, which is coaxially employed with the laser beam through the use of a 1 mm diameter nozzle. The experimenter defined the hyperspace of the experiment before deciding on the experimental design to be used in the present laser cutting experiment by carrying out preliminary tests to identify different combinations of parameters of laser cutting under experimental conditions. To determine the effect of one parameter on the quality of the cut, there is a need to vary that parameter whilst keeping the other parameters constant.

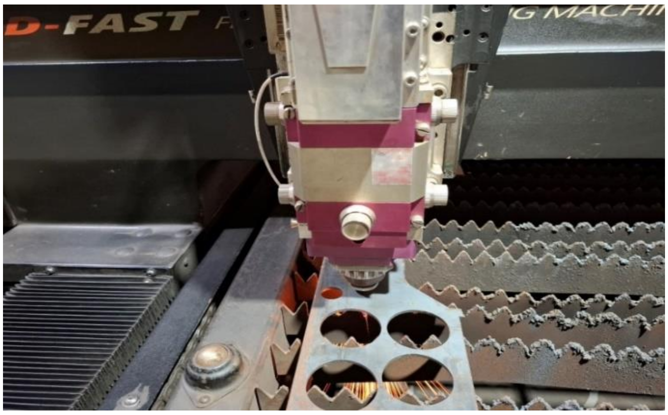

Fig. 2. Laser cutting machine used in the experiment

The tests used the Taguchi approach, which helps to establish the influence of different aspects and then optimize the cutting process. It is divided into two major parts: it defines a set of orthogonal arrays in which to carry out experimentation and provides a common method of interpreting the results. Three distinct input variables have been experimentally examined: LP, GP, and CS. The ranges of these parameters are presented in Table 1.

Table 1: Parameter levels

Factors	Parameters	Levels		
		1	2	3
A	Laser Power (W)	600	800	1000
B	Gas Pressure (bar)	6	8	10
C	Cutting Speed (m/min)	6	12	18

The experiments were structured using a L9 Taguchi mixed-level design. To assess the repeatability of the experimental measurements, three repeated measurements were performed for each of the nine L9 conditions. These repeated measurements were used to estimate the pure-error component in the revised ANOVA. The mean cutting time, kerf width, and surface roughness are presented in Table 2. Laser cuts were executed in a circular orientation on the sheets. The sectioned sample is depicted in Figure 3. Kerf width of the circular laser-cut specimens was determined using the inner–outer diameter method. The outer and inner diameters of the cut profile were measured using a Vernier caliper instrument. Surface quality of the cut edge was measured using a surface roughness tester on the cut edge by considering the average value of roughness. The measurements were made at various positions along the direction of cutting, and the average value was reported in micrometers (µm).

Fig. 3. Laser cut samples

Table 2: Different cut trial parameters

Ex.No	Input Parameters			Output Response (Avg.)		
	LP (W)	GP (bar)	CS (m/min)	Cutting Time (Sec)	Kerf width (mm)	SR (µm)
1	600	6	6	40.107	0.38	9.489
2	600	8	12	20.25	0.33	6.032
3	600	10	18	18.84	0.17	5.245
4	800	6	12	19.052	0.39	8.732
5	800	8	18	18.84	0.32	17.24
6	800	10	6	32.69	0.22	11.318
7	1000	6	18	16.84	0.33	6.044
8	1000	8	6	18.69	0.16	8.932
9	1000	10	12	13.052	0.18	6.594

III. Results and Discussions

Laser cutting is one of the primary power-intensive technologies in the manufacturing industry, using natural resources and causing detrimental environmental effects. Efficient power utilization and enhanced product quality during manufacturing are critical benchmarks for the production industry. Power consumption can be diminished by enhancing SR, as a lower surface polish requires less energy during manufacturing. However, this may lead to more rejects, rework, and time. Consequently, an optimal amalgamation of power and surface polish is requisite for the sustainability performance of the producing industry. The TOPSIS method is utilized for multi-objective optimization. Hwang and Yoon created it so that the selected parameter might get the value that was halfway between the best and worst case scenarios [XXVII-XXXI]. In the TOPSIS methodology, a designated weight is assigned to output replies for the purpose of ranking them. The procedures involved in TOPSIS are outlined below.

Normalized Performance Value

In TOPSIS, the units of all criteria are disregarded and turned into normalized values (rij). It is derived from equation (1). The normalized data are presented in Table 3.

$$r_{ij} = \frac{X_{ij}}{\sqrt{\sum_{i=1}^{m} X_{ij}^2}} \quad i=1,2,3\ldots9;j=1,2,3 \qquad (1)$$

Where,

I = trial count

j = response count

xij= Value of the ith value in the jth experimental trial.

Table 3: Normalized Performance Value

Experiment No	Cutting Time (Sec)	Top Kerf width (mm)	SR (um)
1	0.569286	0.444239	0.332326
2	0.287432	0.385787	0.211254
3	0.267418	0.198739	0.183692
4	0.270428	0.455930	0.305814
5	0.267418	0.374096	0.603783
6	0.464008	0.257191	0.396382
7	0.239030	0.385787	0.211674
8	0.265289	0.187048	0.312819
9	0.185263	0.128596	0.230937

Weighted Normalized Value

As shown in equation (2), multiplying the normalized value by its weights yields the weighted normalized value (vij),

$$vij = wj * rij \qquad i= 1,2,3\ldots9;\ j=1,2,3 \qquad (2)$$

All responses are assigned equal weight. Consequently, wj equals 0.33. Table 4 displays the weighted normalized data.

Table 4: Weighted Normalized Value

Experiment No.	Cutting Time (Sec)	Top Kerf width (mm)	SR (um)
1	0.187864	0.146599	0.109668
2	0.094853	0.127310	0.069714
3	0.088248	0.065584	0.060618
4	0.089241	0.150457	0.100919
5	0.088248	0.123452	0.199249
6	0.153123	0.084873	0.130806
7	0.078880	0.127310	0.069853
8	0.087545	0.061726	0.103230
9	0.061137	0.042437	0.076209

Positive-Ideal (S+) and Negative-Ideal (S-) Solutions

It has been computed using equations (3) and (4),

$$S^{+} = \{(Max\ (v_{ij})\ |\ j \in J),\ (Min\ (v_{ij})\ |\ j \in J')\ |\ i=1,2\ldots9\} \qquad (3)$$

$$S^{-} = \{(Min\ (v_{ij})\ |\ j \in J),\ (Max\ (v_{ij})\ |\ j \in J')\ |\ i=1,2\ldots9\} \qquad (4)$$

Where,

J comprises advantageous traits, while J′ consists of disadvantageous attributes. Table 5 displays the S+ and S- values.

Table 5: Positive-Ideal and Negative-Ideal Solutions

Experiment No.	Cutting Time (Sec)	Top Kerf width (mm)	SR (µm)
1	0.187864	0.146599	0.109668
2	0.094853	0.127310	0.069714
3	0.088248	0.065584	0.060618
4	0.089241	0.150457	0.100919
5	0.088248	0.123452	0.199249
6	0.153123	0.084873	0.130806
7	0.078880	0.127310	0.069853
8	0.087545	0.061726	0.103230
9	0.061137	0.042437	0.076209
S+	0.187864	0.150457	0.060618
S-	0.061137	0.042437	0.199249

The distance of each alternative from the S+ and the S- is determined according to equations (5) and (6).

$$D_i^+ = \sqrt{\sum_{i=1}^{9}(v_{ij} - s_j^+)^2} \qquad (5)$$

I = 1, 2…9.
J=1, 2, 3

$$D_i^- = \sqrt{\sum_{i=1}^{9}(v_{ij} - s_j^-)^2} \qquad (6)$$

Closeness Coefficient Value

The proximity coefficient value for all alternatives (Ci) is computed as demonstrated in equation (7), and the result is shown in Table 6.

$$C_i = \frac{D_i^-}{D_i^- + D_i^+} \qquad (7)$$

Table 6: Closeness Coefficient Value

Experiment No.	D_i^+	D_i^-	Ci	Rank
1	0.049201	0.186908	0.791618	1
2	0.096279	0.158491	0.622094	2
3	0.130870	0.143140	0.522391	6
4	0.106540	0.148751	0.582674	3
5	0.172832	0.085431	0.330791	9
6	0.102150	0.122257	0.544800	5
7	0.111798	0.155761	0.582157	4
8	0.140545	0.101435	0.419187	8
9	0.167247	0.123039	0.423856	7

Average Closeness Coefficient Value

The Taguchi method was employed to determine the optimal parameter levels and the optimal parameters after consolidating several responses into one. The proximity coefficient was utilized to compute the mean effect, as detailed in Table 7.

Table 7: Average Closeness Coefficient Value

Levels	Factors		
	LP (W)	GP (bar)	CS (m/min)
1	0.585202	0.486088	0.475067
2	0.645368	0.542875*	0.478446
3	0.652151*	0.457357	0.497016*

*Indicates optimum level of factors (A3B2C3)

The optimal factor levels, determined by the maximum value in Table 7, are A3B2C3. The optimal conditions consist of a LP of 1000 W, a GP of 8 bar, and a CS of 18 m/s. A LP of 1000 W provides adequate thermal energy to effectively melt and eliminate material during the cutting procedure. Sufficient energy input guarantees consistent cutting conditions and enhances material removal, hence decreasing cutting time while preserving an appropriate kerf width and superior surface quality. The GP of 8 bar is crucial for expelling the molten material from the cutting zone. At this pressure level, the help gas efficiently removes debris and molten particles, yielding a cleaner cutting path. This enhances the cut quality by minimizing inconsistencies along the kerf edges and improving the surface finish. A CS of 18 m/s ensures excellent interface time between the laser beam and the workpiece material. Insufficient cutting speed may result in excessive heat accumulation, causing a larger kerf and suboptimal surface finish. If the speed is excessively high, inadequate energy transfer may lead to incomplete cutting. The chosen speed guarantees effective cutting while preserving surface integrity. The TOPSIS analysis reveals that this combination exhibits the maximum closeness coefficient from the non-ideal solution across all experimental settings. Consequently, this parameter set attains the optimal balance between productivity and cut quality, leading to enhanced overall cutting performance.

Parameter Significance

For the ensuing ANOVA, the TOPSIS proximity coefficient (Ci) derived from Equation (7) was taken into consideration as the sole response variable. A higher Ci value indicates better overall performance when taking into account the combined responses of cutting time, kerf width, and surface roughness. The closeness coefficient shows how close each experimental trial is to the positive-ideal solution. In order to measure the contribution of the input parameters—LP, GP, and CS to the overall multi-response performance, the Ci values acquired for the nine experimental trials were used as the response data in the ANOVA.

Table 8 illustrates the proportional impact of the input parameters determined by the TOPSIS Technique. This study examines LP, GP, and CS as input factors, with performance responses including cutting time, kerf width, and SR. ANOVA is employed to ascertain the significance level of each input parameter and its impact on multiresponse features [XXVII]. The data reveal that GP contributes the most, accounting for 41%, hence exerting the most influence on the overall performance responses. This indicates that fluctuations in gas pressure significantly affect the efficacy of material removal, the quality of the cut, and the resultant surface attributes. LP has the second greatest influence at 37%, underscoring its significant function in regulating the energy imparted to the material. Increased or adjusted laser power influences cutting efficiency and directly affects kerf generation and surface finish. CS accounts for 15%, signifying a moderate influence on the responses. The CS impacts the contact duration between the laser beam and the material; however, its effect is relatively less significant than that of LP and GP. The residual variation represents unexplained variability associated with process fluctuations, experimental factors not included in the model, and model limitations. It should not be directly interpreted as measurement inaccuracy. Since the response values shown in Table 2 are averages from the experimental measurements, this residual variance should not be simply construed as measurement inaccuracy. As a result, the residual term is thought to reflect the combined impact of experimental fluctuations, model restrictions, and unaccounted process variability. Repeated measurements under the experimental settings were used to evaluate the response measures' repeatability, and the observed variance was found to be minimal. Therefore, it is more appropriate to consider the 7.03% residual contribution as unexplained process/model variability rather than measurement error. The TOPSIS-based research indicates that, while CS has very little impact, GP and LP are the primary parameters controlling the overall cutting performance.

Table 8: ANOVA of the TOPSIS closeness coefficient

Source	DoF	Sum of Squares (SS)	Mean Square (MS)	F-value	p-value	Contribution (%)
LP	2	0.171720	0.085860	50388.73	<0.001	37.51
GP	2	0.188146	0.094073	55208.95	<0.001	41.10
CS	2	0.069726	0.034863	20460.04	<0.001	15.23
Lack-of-Fit	2	0.028143	0.014072	8258.31	<0.001	6.15
Pure Error	18	0.000031	0.00000170	-	-	0.01
Total	26	0.457766	-	-	-	100.00

Confirmation Test

After selecting the best parameter levels, the subsequent stage is to forecast and validate the excellence of the quality attribute. The findings of the confirmation test are presented in Table 9. The optimal level setting determined by the studies is A3B2C3. The prediction can be derived from this literature [XXVIII].

Table 9: Confirmation Test Results

Resposnes	Parameters	Predicted	Experimental	Error %
Cutting Time (Sec)	A3B2C3	11.08	11.24	1.43
Kerf width (mm)		0.16	0.15	6.67
Surface Roughness (µm)		4.21	4.32	2.54

The optimization model predicted values were compared to the empirical values of the cutting duration, kerf width, and SR. The expected value was to cut time in 11.08 seconds, but the experimental one was 11.24 seconds, which is a slight error of 1.43

seconds. It means that the model accurately predicts the time of cutting under the optimum conditions. The estimated kerf was 0.16 mm, and the experimental one was 0.15 mm, with a corresponding error of 6.67%. Although the deviance is slightly larger than the other responses, it is in the acceptable range of machining studies. The estimated SR was 4.21 µm, the same as the experimental value of 4.32 µm, which was followed by a margin of 2.54. The high dependence between the experimental and predicted results confirms the reliability of the optimization model. The low percentage differences between the expected and the experimental values are signs that the optimization technique constructed proves to be working and effective in the accurate forecasting of machining performance when under the decided ideal parameters. This will prove the applicability of the optimized parameters to improve cutting performance.

IV. Microstructure Analysis

To examine the surface morphology under optimized and non-optimized cutting circumstances, two laser-cut galvanized iron specimens were subjected to SEM examination. The first specimen is A3B2C3 (LP = 1000 W, GP = 8 bar, and CS = 18 m/min), which is the optimal parameter combination found via the Taguchi-TOPSIS study. For this specimen, 4.32 µm was the measured SR.

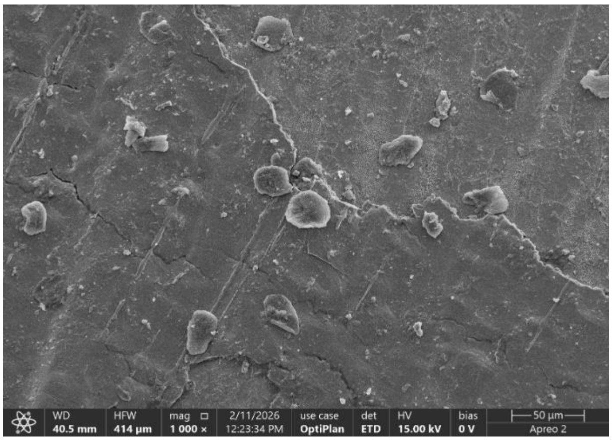

Fig. 7. SEM at Optimized Condition (1000 W, 8 bar, 18 m/min; SR = 4.32 µm)

The SEM morphology of the surface corresponding to the optimal condition is shown in Figure 7. Reduced deposition of re-solidified molten material and a comparatively smooth and uniform cut surface are the results of the optimal condition. Micro-debris and small fragments of shattered materials can be seen scattered all over the surface in the image, formed in the course of the process of removing the material. The presence of such particles means that the cutting parameters influence the effectiveness of the molten material ejection. Besides, the coating layer is galvanized and becomes locally melted and partially vaporized, thus altering the SR and leading to uneven distribution of materials. The surface is relatively smoother and even, and there are not such large deposits of molten matter. Although micro-cracks and scattered re-solidified droplets exist, the distribution of these particles is rather reduced. The grooves and surface markings are less noticeable, indicating quite a stable process of melting and material removal.

For comparison, the second specimen was picked from Experiment 5, with LP = 800 W, GP = 8 bar, and CS = 18 m/min, with a measured surface roughness of 17.24 µm. This condition was chosen because the gas pressure and cutting speed are the same as those in the optimal condition, but the laser power is reduced from 1000 W to 800 W. Thus, the comparison assesses the effect of laser power on the resulting surface morphology.

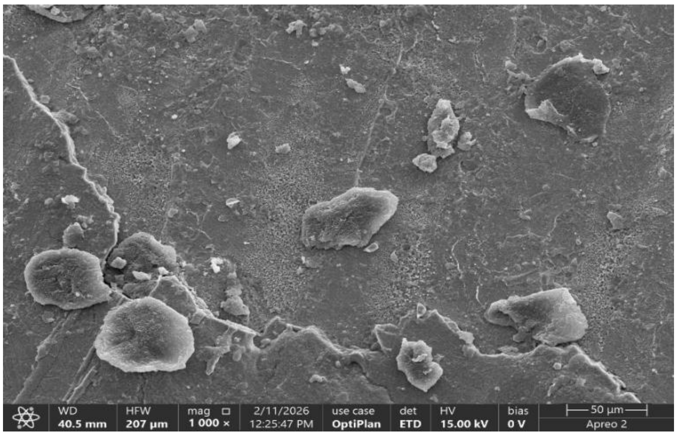

Fig. 8. SEM Micrograph at Comparative Condition (800 W, 8 bar, 18 m/min; SR = 17.24 µm)

The SEM micrograph of the galvanized iron surface created with 800 W laser power, 8 bar gas pressure, and 18 m/min cutting speed is shown in Figure 8. The surface roughness was measured to be 17.24 µm. The micrograph shows an imbalanced surface morphology where the melted and re-solidified particles were observed throughout the cutting region. The laser cutting method involves the use of high power beam of laser that generates concentrated heat that melts the material following the cutting path. When the assist gas pushes out the molten metal, some of the molten material would re-solidify on the surface, forming globular droplets and irregular clusters. These properties are clearly shown in the picture, indicating the high rate of melting and solidification. Compared with the optimized condition, the surface exhibits more irregularities, re-solidified particles, and molten material deposits. These features indicate less uniform material removal and are consistent with the higher surface roughness measured for this condition.

V. Conclusion

This study employed the Taguchi technique in conjunction with TOPSIS to optimize the laser-cutting parameters of galvanized iron sheets. The obtained results of the experiment proved that the TOPSIS technique was an efficient method of converting the different response features into one closeness coefficient that helped to select the best set of cutting parameters. The analysis revealed that the optimal parameter combination is an LP of 1000 W, GP of 8 bar, and CS of 18 m/min. This parameter combination provided the best trade-off between productivity and cut quality. The contribution study showed that the most important parameter was the gas pressure at 41%, next was LP at 37%, and the last was CS at 15% to the overall cutting performance. The confirmation test showed that there was a high correlation between the predicted and experimental values, and errors on the cutting time, kerf width, and SR were 1.43 per cent, 6.67 per cent, and 2.54 per cent, respectively, therefore establishing the reliability of the optimization method. In addition, SEM microstructural examination has also been performed in order to compare surface morphology under optimum and non-optimized cutting conditions. The best condition exhibited a smoother and more homogeneous surface and fewer re-solidified particles with less deposition of molten material. In contrast, the non-optimized condition exhibited an irregular surface morphology, larger molten droplets, and increased surface defects.

Conflict of Interest:

The authors declare that there was no relevant conflict of interest regarding this paper.

References

I. Alsaadawy, Muhammad, et al. "A Comprehensive Review of Studying the Influence of Laser Cutting Parameters on Surface and Kerf Quality of Metals." The International Journal of Advanced Manufacturing Technology, vol. 130, nos. 3–4, 2024, pp. 1039–1074. 10.1007/s00170-023-12768-1.

II. Alsaadawy, Muhammad, et al. "Investigation of the Effect of Laser Cutting Parameters on Surface and Kerf Quality of Thick Ti–6Al–4V Alloy Sheets." Arabian Journal for Science and Engineering, 2024, 10.1007/s13369-024-09083-6.

III. Arifin, Mohammad Danil, and Moch Ricky Dariansyah. "Lifespan Estimation of Galvanized Steel and Stainless Steel Pipe." International Journal of Marine Engineering Innovation and Research, vol. 8, no. 3, 2023, pp. 468–476. 10.12962/j25481479.v8i3.18650.

IV. Dey, Joydeep, and Ankur Bansod. "Effect of Doping on Thermo-Optical Properties of Vanadium Oxide Sputtered Thin Films." Materials Today: Proceedings, vol. 37, 2021, pp. 580–83. 10.1016/j.matpr.2020.05.593.

V. Dhanaraj, P. S., and C. Rathinasuriyan. "Optimization of Fiber Laser Welding Parameters for High Strength Aluminium Alloy AA7075-T6." Materials Today: Proceedings, vol. 52, 2022, pp. 283–89. 10.1016/j.matpr.2021.08.276.

VI. Dhanaraj, P. S., and C. Rathinasuriyan. "Selection of Intense Energy Welding Process for High Strength Aluminum Alloy Using AHP." Materials Today: Proceedings, vol. 46, 2021, pp. 8254–59. 10.1016/j.matpr.2021.03.245.

VII. Eriksen Hammer, Stine, et al. "Characterisation of Particles Emitted during Laser Cutting of Various Metal Sheets and an Exposure Assessment for the Laser Operators." International Journal of Environmental Research and Public Health, vol. 19, no. 16, 2022, p. 9888. 10.3390/ijerph19169888.

VIII. Hamoda, Ahmed, et al. "Experimental and Numerical Analysis of Deep Beams with Openings Strengthened with Galvanized Corrugated and Flat Steel Sheets." Case Studies in Construction Materials, vol. 21, no. e03522, 2024, p. e03522. 10.1016/j.cscm.2024.e03522.

IX. Hasan, H. K. "Analysis of the Effecting Parameters on Laser Cutting Process by Using Response Surface Methodology (RSM) Method." Journal of Achievements in Materials and Manufacturing Engineering, vol. 110, no. 2, 2022, pp. 59–66. 10.5604/01.3001.0015.7044.

X. Kechagias, J. D., et al. "An Investigation of Surface Quality Characteristics of 3D Printed PLA Plates Cut by CO2 Laser Using Experimental Design." Materials and Manufacturing Processes, vol. 36, no. 13, 2021, pp. 1544–53. 10.1080/10426914.2021.1906892.

XI. Khoshaim, Ahmed B., et al. "Experimental Investigation on Laser Cutting of PMMA Sheets: Effects of Process Factors on Kerf Characteristics." Journal of Materials Research and Technology, vol. 11, 2021, pp. 235–46. 10.1016/j.jmrt.2021.01.012.

XII. Kumar, Senthil Velukkudi Santhanam, Lokesh Rathinaraj, Rathinasuriyan Chandran, and Sankar Ramaiyan. "Multi Response Optimization of Submerged Friction Stir Welding Process Parameters Using TOPSIS Approach." ASME 2015 International Mechanical Engineering Congress and Exposition, vol. 2B, 2015. 10.1115/IMECE2015-50353.

XIII. Ma, Guohong, et al. "A Vision-Based Method for Lap Weld Defects Monitoring of Galvanized Steel Sheets Using Convolutional Neural Network." Journal of Manufacturing Processes, vol. 64, 2021, pp. 130–39. 10.1016/j.jmapro.2020.12.067.

XIV. Madić, Miloš, et al. "Application of a Robust Decision-Making Rule for Comprehensive Assessment of Laser Cutting Conditions and Performance." Machines, vol. 10, no. 2, 2022, p. 153. 10.3390/machines10020153.

XV. Najjar, I. M. R., et al. "Predicting Kerf Quality Characteristics in Laser Cutting of Basalt Fibers Reinforced Polymer Composites Using Neural Network and Chimp Optimization." Alexandria Engineering Journal, vol. 61, no. 12, 2022, pp. 11005–18. 10.1016/j.aej.2022.04.032.

XVI. Rachieru, Nicoleta. "Risk Prioritization in the Laser Cutting Process Using the FMEA Method Compared to the TOPSIS Method." RECENT Journal, vol. 25, no. 2 (73), 2024, pp. 122–129. 10.31926/RECENT.2024.73.122.

XVII. Ramaiyan, Sankar, Udayakumar Mani, Rathinasuriyan Chandran, and Senthil Kumar V. S. "Optimization of Corrosion Behavior in Submerged Friction Stir Processed Magnesium AZ31B Alloy." ASME 2017 International Mechanical Engineering Congress and Exposition, vol. 2, 2017. 10.1115/IMECE2017-72559.

XVIII. Rana, R. S., et al. "Optimization of Process Parameter of Laser Beam Machining of High Strength Steels: A Review." Materials Today: Proceedings, vol. 5, no. 9, 2018, pp. 19191–99. 10.1016/j.matpr.2018.06.274.

XIX. Rathinasuriyan, C., and V. S. Senthil Kumar. "Optimisation of Submerged Friction Stir Welding Parameters of Aluminium Alloy Using RSM and GRA." Advances in Materials and Processing Technologies, vol. 7, no. 4, 2021, pp. 696–709. 10.1080/2374068x.2020.1793264.

XX. Shreyas, P., et al. "Mechanical Properties and Microstructure of 316L-Galvanized Steel Weld." Materials Today: Proceedings, vol. 23, 2020, pp. 600–07. 10.1016/j.matpr.2019.05.418.

XXI. Siengchin, Suchart. "A Review on Lightweight Materials for Defence Applications: Present and Future Developments." Defence Technology, vol. 24, 2023, pp. 1–17. 10.1016/j.dt.2023.02.025.

XXII. Singh, Yadvinder, et al. "Multi-Objective Optimization of Kerf-Taper and Surface-Roughness Quality Characteristics for Cutting-Operation on Coir and Carbon Fibre Reinforced Epoxy Hybrid Polymeric Composites during CO2-Pulsed Laser-Cutting Using RSM." Lasers in Manufacturing and Materials Processing, vol. 8, no. 2, 2021, pp. 157–82. 10.1007/s40516-021-00142-6.

XXIII. Singh, Yadvinder, et al. "Process Parameter Optimization in Laser Cutting of Coir Fiber Reinforced Epoxy Composite—A Review." Materials Today: Proceedings, vol. 48, pt. 5, 2022, pp. 1021–1027. 10.1016/j.matpr.2021.06.344.

XXIV. Trajković, Aleksandar, and Miloš Madić. "Application and comparison of MCDM methods for the assessment of fiber laser cutting." Innovative Mechanical Engineering 2.3, 2023. https://orcid.org/0000-0002-2310-2590.

XXV. Wang, Hong-Jian, and Tao Yang. "A Review on Laser Drilling and Cutting of Silicon." Journal of the European Ceramic Society, vol. 41, no. 10, 2021, pp. 4997–5015. 10.1016/j.jeurceramsoc.2021.04.019.

XXVI. Xie, Zhiqiang, et al. "Study on Shear Performance and Calculation Method for Self-Pierce Riveted Joints in Galvanized Steel Sheet." Thin-Walled Structures, vol. 161, no. 107490, 2021, p. 107490. 10.1016/j.tws.2021.107490.

XXVII. Yao, YanSheng, et al. "Experimental study on laser cutting process of titanium–zirconium amorphous alloy." AIP Advances 14.1, 2024. 10.1063/5.0188219.

XXVIII. Yuvaraj, N., and M. Pradeep Kumar. "Multiresponse Optimization of Abrasive Water Jet Cutting Process Parameters Using TOPSIS Approach." Materials and Manufacturing Processes, vol. 30, no. 7, 2015, pp. 882–89. 10.1080/10426914.2014.994763.

XXIX. Vasudevan, A., Sam, T. H., Raman, A., RATANAKVISAL, Fei, Z., & Ng, C.-P. (2022). The effective implementation of the 5s concept on the performance: A case study of a manufacturing company in Malaysia. 10.5281/ZENODO.6956027

XXX. Zubairuddin, M., Ravi kumar, R., Chaursaia, P. K., & Ali, B. (2021). Thermo-mechanical analysis of laser welding of Grade 91 steel plates. Optik, 245(167510), 167510. 10.1016/j.ijleo.2021.167510

XXXI. Zubairuddin, M., Vasudevan, M., Elumalai, P. V., Akram, M., Attar, P. R., & Krishnasamy, E. (2026). Numerical and experimental analysis of temperature and residual stress of GTA and LASER welding for grade 91 steel. International Journal on Interactive Design and Manufacturing (IJIDeM), 20(9), 5137–5149. 10.1007/s12008-024-02138-w